COMPARISON STUDIES OF R-CURVES FOR FATIGUE AND TEAR CRACKS IN A THIN ALUMINIUM PLATE

V.P.Naumenko[1], G.S.Volkov[1] and A.G.Atkins[2]

[1] Department of Modelling and Fracture, Institute for Problems of Strength
Timiryazevskaya Str.2, 01014, Kyiv, Ukraine
[2] Department of Engineering, The University of Reading
Whiteknights, Reading, RG6 6AY, UK

ABSTRACT

In this work we are searching for an explanation of some qualitative distinctions between global and local R-curves expressed in terms of the stress intensity factor, K_R, and the crack-tip opening angle, ψ_R. The R-curves are determined for fatigue and tear precracks in the same low-constraint geometry tested under uniaxial tension. The fracture analysis is focused on the steady-state process wherein some extreme points on a crack profile are continuously displacing in proportion to an increment of the net-section stress. The whole response of the center-cracked specimen is predominantly elastic for each set of test parameters. The crack-tip plastic zones are small as compared with the sizes of the crack length and specimen ligament, and yet they are large in comparison with the specimen thickness. Consequently, the fracture behaviour can be treated as elastic governed by the K_R resistance and at the same time as elastoplastic governed by the ψ_R resistance.

INTRODUCTION

The R-curve concept is designed for predicting the residual strength of damage-tolerant structures subjected to monotonously increasing loads without much regard to load-precracking history effects. However, these effects may take great significance, say, for assessing cracks in aging aircraft components made from Al-alloys and other metallic materials. A strong influence of the cyclic crack growth history on fracture toughness was reported in [1] for aluminum alloy 2024-T3, in [2] for D6AC steel, and in [3] for TP304 stainless steel and A106 Grade B carbon steel. Even a cursory examination of these and other references demonstrates that the phenomenon in question is rather complicated and incomprehensible. That is why this work is targeted at studying the relatively simple special case of a large amount of stable crack extension under plane stress conditions. To be specific, long straight-through cracks in a large-scale M(T) specimen made of a thin-sheet aluminum alloy are considered in what follows.

It is well known that the J-integral fracture criterion begins to show a configuration dependence for large crack extensions in thin ductile materials. A criterion that does not suffer supposedly from this limitation is the constant ψ_{ss} angle.The test data are also analyzed in terms of K_R, as the stress intensity K_I is the only crack-driving parameter, which can be easily and accurately calculated both for stationary and growing cracks. In such a manner we intend to demonstrate that the current practice for the R-curve determination needs essential refining. Some new possibilities for an alternative characterization of the crack-extension resistance are offered.

BACKGROUND

An actual crack border provides the basis for much of the methodology used in this study. To characterize a stationary crack in a comprehensive way, we have to know the initial crack profile related to a zero level of the crack-tip stress σ_l. This crack-tip event is specified by subscript "e" for the following parameters: the initial values of the crack length, $2c_e$, the crack-mouth opening spacing, $2h_e$, and the crack-tip opening spacing, δ_{te}, (Fig.1a). In addition, the elastic compliances of the crack border in its extreme points x = 0, y = $\pm$ h_e (transverse direction) and x = $\pm$c, y = $\pm$0.5 δ_{te} (longitudinal direction) are to be determined. The crack-tip "tt" is represented in Fig.1 by a vertical line passing through the point x = c. To define the δ_t value, the procedure of extrapolating the 2h(x)-curves in the range $x > x_n$ is employed. Here d_s is a fixed distance from the observed crack-tip taken as a first approximation, to be d_s =0.5 B, where B is the specimen thickness.

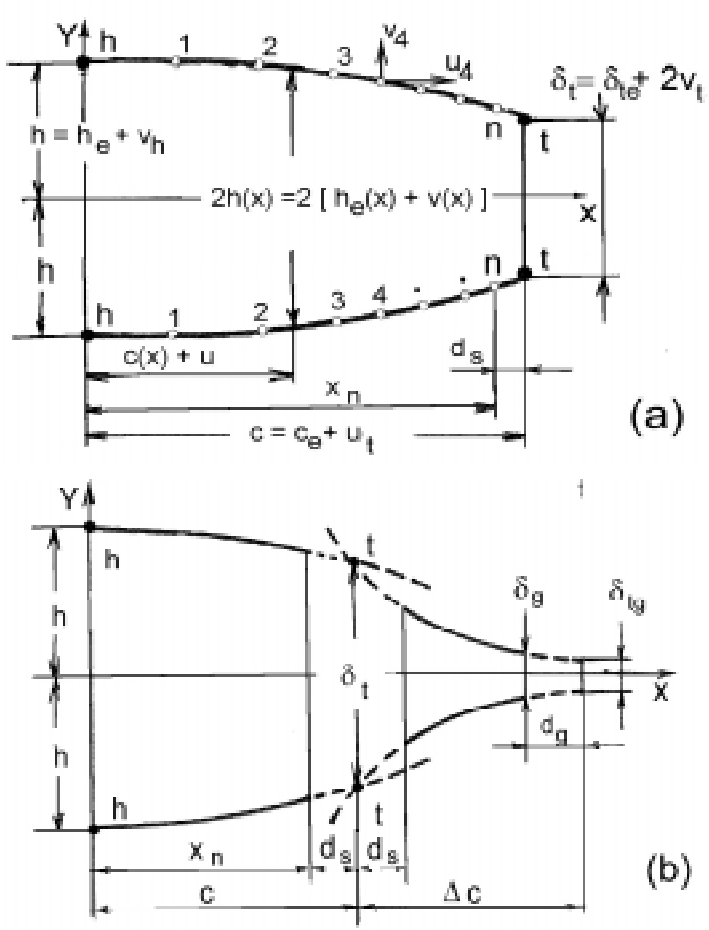

Figure 1: Schematic sketches of the center crack profile in the course of crack-tip blunting (a) and slow-stable ductile tearing (b)

During the initial stages of stable crack extension, the geometry of the near-tip crack border changes drastically (Fig.1b). After stable crack extension greater than about B, however, the profile of the growing crack in the range (c + B) < x < (c + Δc) always appears as convex down. At the same time, the crack border in the range x < c remains convex up. The shape of the near-crack-tip profile is uncertain when $\Delta c < B$. Additionally, there is uncertainty in the region near the observed tip of a steadily growing crack.. In our case, the δ_{tg} value could not be distinguished reproducibly from zero. That is why the crack opening spacing δ_g measured at the specified distance d_g= 0.5B is used as the local crack-driving parameter. The averaged ψ value is defined, on the assumption of δ_{tg} =0, as

$$\psi = 2 \tan^{-1} (\delta_g / 2d_g) \quad (1)$$

EXPERIMENTAL PROCEDURE

The test material is aluminium 1163 AT in the as-received condition. This is a high-strength aero-skin alloy similar to Al 2024-T351. A specimen is made such that the applied stress σ is parallel to the rolling direction of the sheet. Sheet-type specimens were fabricated and tested as prescribed by the ASTM Standard Method for Tension Testing of Metallic Materials (E8M-85). The tensile properties of the alloy under ambient conditions are: elastic modulus E=73 GPa, 0.2% offset yield stress σ_Y = 334 MPa, the ultimate strength σ_u= 446 MPa, and the flow stress $\sigma_o = 0.5 (\sigma_Y + \sigma_u)$ = 390 MPa. The true stress, σ_t vs true strain, ε_t, curve is well approximated by the relation

$$\sigma_t = K (\varepsilon_t)^N \quad (2)$$

with K =631 MPa and N = 0.113.

A fatigue precrack of length 2c = 508 mm was grown in an M(T) specimen of width 2W = 1200 mm, height 2H = 2760 mm and thickness B = 1.05 mm. Precracking was performed under constant amplitude cyclic loading at the stress ratio R = 0.4 and the maximum stress in the net section σ_N near 55 MPa, thus satisfying the commonly accepted requirements on fatigue precracking. The maximum K_I value under cyclic loading K^f_{max} = 32 MPa. Tests were conducted in accordance with the requirements of the ASTM Standard Practice for R-curve Determination (E 561-92a), including some special developments in the test procedure to eliminate uncontrolled or spurious stress distributions in the specimen. Undesirable buckling and friction effects were not sufficient to cause significant test errors. Stable tearing was initiated in the fatigue pre-cracked test piece. The cracking was terminated by complete unloading. It should be noted that at the onset of unloading at σ_N = 302 MPa the tear crack continued to grow until it stopped at $\sigma_N \approx$ 251 MPa when reaching the length 2c = 542 mm. The related K_I value denoted K^t_{max} is equal 158 MPa$\sqrt{m}$. Two other tests were performed to determine the K_R curves of the material but in these two tests, the different length starter cracks (542 and 578mm) were not pre-fatigued but were merely the result of some previous stable tearing. For the third test K^t_{max} = 146 MPa$\sqrt{m}$.

In the course of fracture tests the specimens were loaded incrementally, allowing the time between steps for the crack to stabilize before measuring the load, crack length, and crack border profile. To develop R-curves with confidence, we usually assigned more than fifteen steps (data points) for each test condition. Once the crack had been stabilized within seconds of stopping the loading, a close-up photograph of the near-crack-tip profile [x > (c - 7 mm)] was taken (on which Fig.1 is based). Four diagrams: load P versus crack-mouth opening displacement $2v_h$; load P versus problem domain displacement $2v_d$; load P versus load-point displacement $2v_P$; and load P versus crack-tip opening spacing δ_t, were recorded simultaneously (Fig.2).

RESULTS

First, we investigate K_R as a relevant measure of fracture resistance. The plastic-zone adjustment r_Y recommended by Practice E561 is calculated with the use of the flow stress σ_o. Pronounced differences are observed between the K_R-curves for the fatigue and tear precracks (Fig.3). In all the cases the P vs $2v_P$ diagram was almost linear not only for a stationary crack, but it was also nearly linear throughout the entire range $0 < \Delta c < 10.5$ mm. Nevertheless, the selection of K as the governing crack-driving parameter with no regard for residual stress-strain fields, crack-closure, crack-tip necking and other local phenomena is, strictly speaking, invalid.

The load P vs crack-tip opening spacing δ_t diagram shown in Fig.2 is considered fundamental. It carries a considerable body of information on the near-crack-tip zone in its true value. As the point, where transverse displacement v(x,y) is measured, moves away from the crack-tip, the above information is less readily

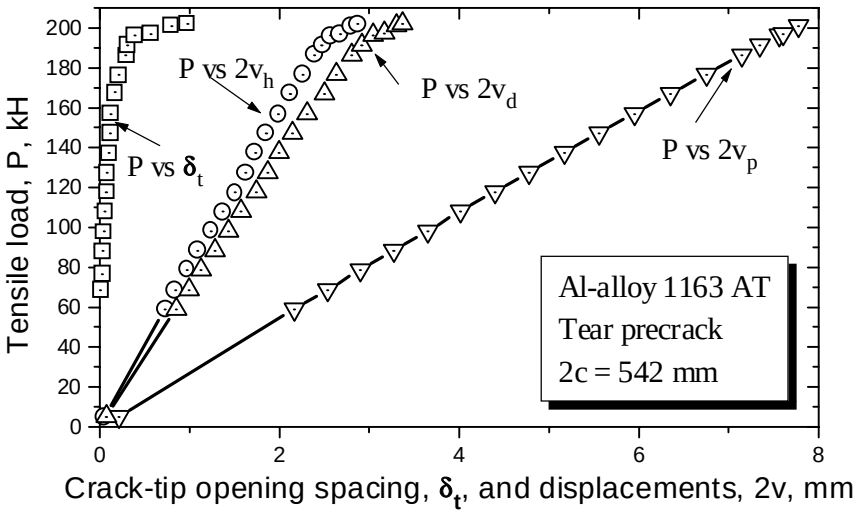

Figure 2: Test records with markers made simultaneously at every loading step.
The coordinates of the measurement points are:
δ_t (x = c, y = ± δ_{te}); v_h (x = 0, y = ± h_e); v_d (x = 0, y = ±108 mm); v_p (x = 0, y = ±1380 mm)

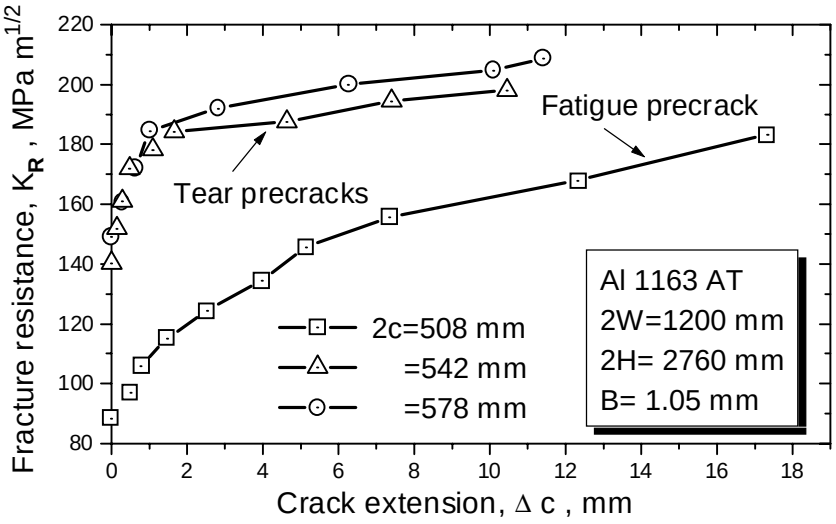

Figure 3: Global R-curves for the fatigue and tear precracks in the same M(T) specimen

available. Such loss is much more pronounced for a tear crack than for a fatigue one. In both cases, the basic test record P vs δ_t is more responsive to changes in the loading history and in the near-crack-tip plasticity than any other test record. The observed nonlinearity of the basic diagrams is associated with very large values of the ratio r_Y / B for the growing cracks.

To ensure an adequate correlation of the fracture toughness quantities related to the different starting conditions of the precracks (i.e., fatigue and tear precracks), we start with the set of near-crack-tip profiles shown in Fig.4, which also may be treated as the set of experimental diagrams recorded at different distances from the original position of the crack tip. As the intervals of measurement approach the crack tip, the non-linearity of the diagram comes into particular prominence. Eventually the crack-tip diagram σ_N versus δ_t may be presented by two well-defined straight lines connected by a monotonically rising curve. These lines intersect at point "s" considered as an imaginary start of the steady-state crack growth when the crack-tip spacing increment as well as the crack length increment are in one-to-one proportion to the increment of the net-section stress. The fictitious point "s" may also be defined with the use of the σ_{NR}-curve, that is, the net-section stress σ_N versus crack extension Δc diagram or simply with the use of σ_N vs v_h diagram. Another crack-tip event of interest relates to a zero crack-tip stress σ_l. It is defined as the point "e" on the

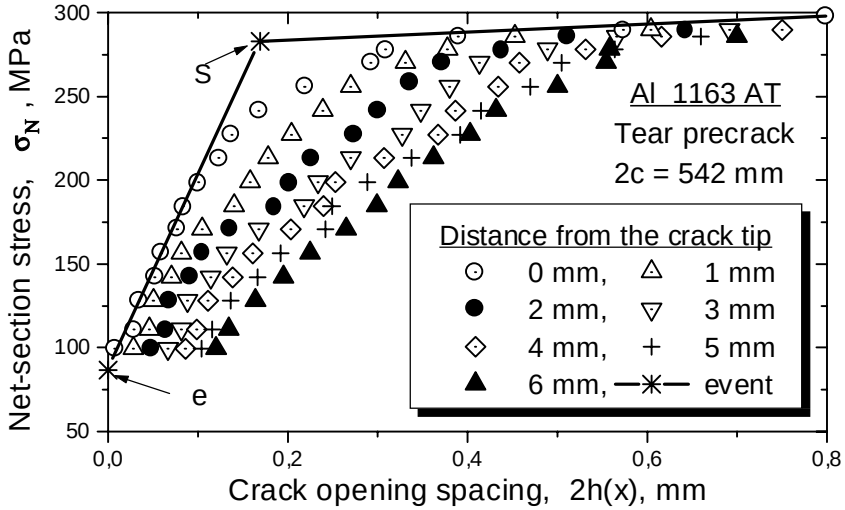

Figure 4: Crack-border spacings on different loading steps
and different distances from the crack-tip position in the M(T) specimen

experimental diagram σ_N vs δ_t (see Fig.4). In this way the initial value of the crack-tip spacing, δ_{te}, is taken as zero. The load σ_{Ne} may be treated as the ordinary crack-tip opening load $(\sigma_N)_{op}$ determined as above.

To eliminate the effects of the load precracking history on fracture toughness, we use the procedure proposed by Newman et al. [2]. They found that the difference between K_R and K_{op} (K_e) (the effective elastic fracture toughness) is nearly constant for a wide range of fatigue pre-cracking stress-intensity factor levels. As can be seen from Fig.5a, the effective values

$$K_R^* = \sigma^* \{\pi (c + r_Y) \sec [\pi (c + r_Y) / 2 W]\}^{0.5}, \quad (3)$$

where $\sigma^* = \sigma - \sigma_e$ for the fatigue and tear precrack starting conditions, are still as far apart as in Fig.3. Our result is supported (but only partially) by the K_R-curves in Fig.5b for 2024-T3 aluminum alloy taken from [1]. Here we use the tensile load P versus Δc diagram taken from [1] and the K_{op} values calculated from the crack-closure model [4]. Those calculations [5] are based on the assumption that for the material under investigation the constraint fitting factor $\alpha \approx 2$.

For both 1163 AT and 2024-T3 aluminum alloys their K_R- and K_R^*-curves continue to increase. In physical terms this implies that the fracture toughness of the materials is limited only by the sizes of the crack and the specimen. On the other hand, the local R-curves for the fatigue and tear precracks are a decreasing function of the crack extension (Fig.6). They have near a "plateau value" of fracture resistance ψ_{ss} which is usually related to the steady-state stage of slaw-stable crack extension. Qualitatively similar ψ_R-curves are presented in [1] for Al 2024 -T3. The plateau values ψ_{ss} are compared in Table 1.

ANALYSIS - DISCUSSION

Large distinctions between the K_R- and K_R^*-curves for fatigue and tearing precracks could not be explained readily through employment of the two-parameter K-T approach. Here we deal with a correlation of two different constraint-related issues. On the one hand, there is a loss of constraint, (that is, reduction in tensile opening stress) under increasing plastic flow for a stationary crack [6, 7], and on the other one, an increase in tensile opening stress found for a growing crack; a conclusive analysis showing constraint elevation under steady-state crack extension has been carried out by Varias and Shih [8].

Nowadays it is generally agreed that the constant ψ_{SS} angle is a more fundamental criterion value than the K_R or J_R resistance for thin-sheet materials. Crack-closure and plasticity effects are less complicated in thin

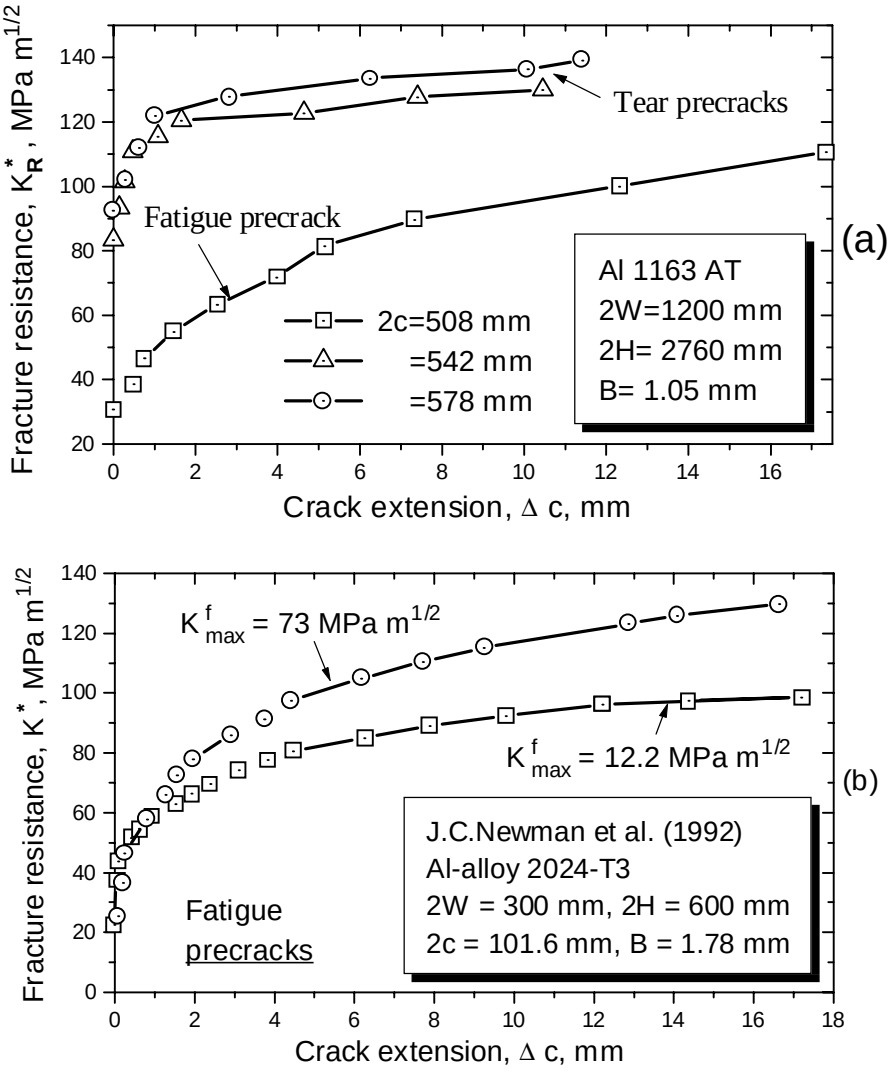

Figure 5: Effective K_R-curves for fatigue and tear precracks in M(T) specimens made of the aluminum alloy sheets

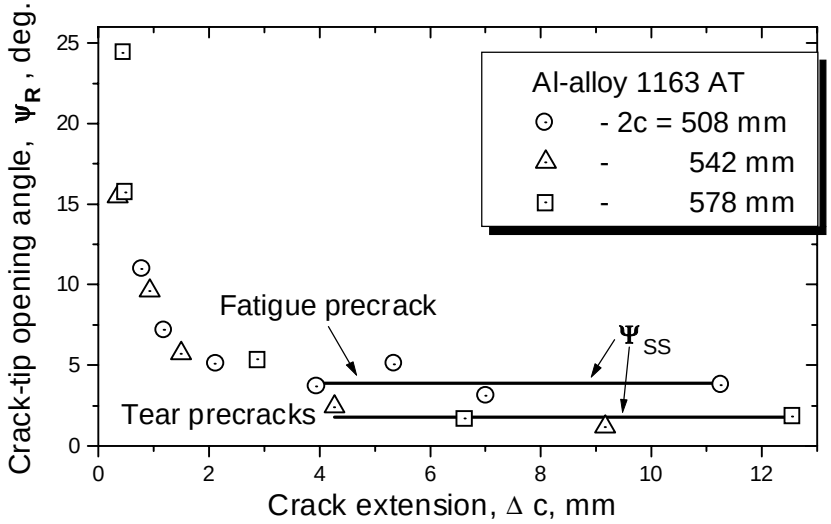

Figure 6: Local R-curves for fatigue and tear precracks in the same M(T) specimen

plates because constraint effects appear to be less important. The computational approach of Newman et al. [1] used with the ψ_{SS} criterion is able to predict the effects of specimen size and precracking stress history on stable tearing. In searching for a simpler alternative approach we turn our attention to the so-called Unified

Methodology (UM) [9, 10]. It is anticipated that the UM, representing a simplified semi-analytic fracture analysis, has the advantage of an appropriate engineering approximation.

TABLE 1
TEST PARAMETERS RELATED TO THE PRECRACKS UNDER CONSIDERATION

Material	Al 1163 AT			AL 2024-T3	
Parameter (units)	Precrack				
	Fatigue,R=0.4 K^f_{max} 32.0 MPa√m	Tear, R = 1 K^t_{max} 158 MPa√m	Tear, R = 1 K^t_{max} 146 MPa√m	Fatigue, R=0 K^f_{max} 12.2 MPa√m	Fatigue, R=0 K^f_{max} 73.0 MPa√m
c_s (mm)	255.8	271.6	290.2	51.5	51.1
σ_{Ns} (MPa)	215.4	283.4	295.5	343.4	364.6
σ^*_{Ns} (MPa)	119.6	196.4	210.6	328.3	286.9
r^*_s (mm)	5.0	14.92	17.4	18.6	12.1
K^*_s (MPa√m)	69.0	119.5	129.0	118.3	95.2
C_{ls}	61.8	74.3	81.4	-	-
ε^*_{ls}	0.435	1.353	1.63	-	-
σ^*_{ls} (MPa)	574.0	652.5	666.5	-	-
α_{ls}, α	1.47	1.67	1.71	1.8[a]	1.8[a]
ψ_{ss} (deg)	3.9	1.8	1.8	6.5[b]	6.5[b]

[a] A single value presentation of the constraint fitting parameter α taken from [4].
[b] An average value related to the distance d_g = 1 mm (see Fig.1b) taken from [1].

The fatigue and tear cracks with a zero crack-tip stress σ_l are represented in the analysis by an elliptic hole. The minimal radius ρ_e = 0.262 mm of the hole is treated as a characteristic of any center crack (c >> B) in a plate of a given thickness made from Al 1163 AT. According to the analysis developed by Neuber [11], the true local strain, ε_l^*, and the true local stress, σ_l^*, at the tips of a hole can be defined as

$$\varepsilon_l^* = \{[C_l \sigma^* (1 + \sigma_N^*/E)]^2 / E K\}^{1/(1+N)}, \quad (4)$$

$$\sigma_l^* = K (\varepsilon_l^*)^N, \quad (5)$$

where C_l is the elastic stress concentration factor. The similarity of Eqs. (5) and (2) is justified by assuming plane stress at the hole tips. Expressions (4) and (5), as applied to the steady-state fracture give the results presented in the Table 1 together with the related C_l values. For a larger tear precrack, the local constraint factor $\alpha_{ls} = \sigma^*_{ls}/\sigma_o$ is close to the constraint fitting parameter α introduced by Newman [4].

To correlate the test parameters for the fatigue and tear precracks we consider an empirical criterion for an imaginary start of self-similar crack propagation in the form

$$W = W_s = \int_0^{\varepsilon_{ls}} \sigma_l d\varepsilon_l = \int_0^{\varepsilon_{le}} \sigma_l d\varepsilon_l + \int_0^{\varepsilon^*_{ls}} \sigma_l d\varepsilon_l , \quad (6)$$

where W_S is the strain energy density at the crack tip on the plane of crack extension. Combining Eqs. (6) and (5) gives

$$W_s = \frac{K}{1+N}\left[\varepsilon_{le}^{1+N} + \left(\varepsilon_{ls}^{*}\right)^{1+N}\right] \quad . \tag{7}$$

This relationship emphasizes the fundamental importance of the following conclusion [12] - the history of the stress and strain in critical regions has to be known accurately, particularly if necking is involved. The first term in the right-hand side of Eq. 7 is not zero for any actual crack. The procedure and results of evaluating the initial strain ε_{le} is beyond the scope of this paper. Nevertheless, going along this line of thinking, we have every reason to believe that the difference between the ψ_{ss} values for the fatigue and tear precracks (Fig.6 and Table) could be explained convincingly.

CONCLUDING REMARKS

It appears as if the concepts of global and local R-curves are both developed on the following tacit assumption – actual structures are subjected to just one monotone load application during their whole life-time. This assumption is in complete contrast to the following commonly accepted statement: to be of value, any fracture criterion and any measure of ductile-tear resistance must be capable of predicting failure strains and stresses under entirely different loading histories. There are strong evidences that the correlation of K_R- and ψ_R-curves has never been considered as the main objective of an experimental study. For thin sheets of Al-alloy 2024-T3, the crack-extension data obtained in [13] on the largest structural panels that have ever been tested are presented solely in terms of K_R. Fairly good fracture predictions for panels with single site and multiple site cracks are made without any reference to available measurements of the crack-tip opening angle for the same set of specimens. These and many similar facts might help to speculate (but not explain) why all our attempts to correlate the K_R- and ψ_R-curves were doomed to failure.

ACKNOWLEDGEMENTS

The co-operation with Drs. O. Kolednik, N. P. O'Dowd, A. I. Semenets, and G. I. Hanin is gratefully acknowledged.

REFERENCES

1. Newman, J.C.,Jr., Dawicke, D.S. and Bigelow, C.A. (1992). In: *Proceedings of the International Workshop on Structural Integrity of Aging Airplanes,* pp. 167-186, Atlanta, Georgia.
2. Newman, J.C., Jr., Bland, J.D. and Berry, R.F.,Jr. (1995). In: *Fracture Mechanics: 26th Volume, ASTM STP 1256,* 23 p., Reuter, W.G., Underwood, J.H. and Newman, J.C., Jr. (Eds). ASTM, Philadelphia.
3. Rudland, D.L. and Brust, F. (1997). In: *Fatigue and Fracture Mechanics: 27th Volume, ASTM STP 1296,* pp. 406-426, Piasciak, R.S., Newman, J.C. and Dowling, N.E. (Eds). ASTM.
4. Newman,J.C.,Jr. (1984). *Int. J. Fract., **24,*** p.R131.
5. Newman, J.C., Jr., Poe, C.C., Jr. and Dawicke, D.C. (1990). In: *Fatigue 90,* Vol.4, pp.2407-2416, Kitagava H. and Tanaka T. (Eds), Birmingham, UK.
6. Betegon,C. and Hancock, J.W. (1991). *J. Appl. Mech., **58,*** p.104.
7. O'Dowd, N.P. and Shih, C.F. (1991). *J. Mech. Phys. Solids, **39,*** p.989.
8. Varias, A.G. and Shih, C.F (1993). *J. Mech. Phys. Solids, **41,*** p.835.
9. Naumenko, V.P. (1998). In: *Fracture from Defects,* Vol.2, pp.1083-1088, Brown, M.M., de los Rios, E.R. and Miller, K.J. (Eds), Sheffield, UK.
10. Naumenko, V.P. (2000). To be published in: *Mechanics of Solids in Russia and Ukraine,* G.S.Pisarenko (Ed.), Znanie, Moscow.
11. Neuber, H. (1961). *J. Appl. Mech., Dec.,* p.544.
12. Atkins, A.G. (1997). In: *Fracture Research in Retrospect,* pp.327-350, Rossmanith, H.P. (Ed.), A.A.Balkema/Rotterdam/Brookfield.
13. de Wit, R., Fields, R.J., Low, S.R., Harne, D.E. and Foecke, T. (1997). In: *Fatigue and Fracture Mechanics: 27th Volume, ASTM STP 1296,* pp. 451-468, Piasciak, R.S., Newman, J.C. and Dowling, N.E. (Eds), ASTM.